Synthesis, Structure−Activity Relationships, and RARγ−Ligand Interactions of Nitrogen Heteroarotinoids

Arindam Dhar,[†] Shengquan Liu,[‡] Jozef Klucik,[‡] K. Darrell Berlin,*[,‡] Matora M. Madler,[‡] Shennan Lu,[†,⊥] R. Todd Ivey,[†] David Zacheis,[▽] Chad W. Brown,[‡] E. C. Nelson,[||] Paul J. Birckbichler,[§] and Doris M. Benbrook*[,†,⊥]

Departments of Obstetrics & Gynecology, of Biochemistry & Molecular Biology, of Otorhinolaryngology, and of Urology, University of Oklahoma Health Sciences Center, P.O. Box 26901, Oklahoma City, Oklahoma 73190, and Departments of Chemistry and of Biochemistry & Molecular Biology, Oklahoma State University, Stillwater, Oklahoma 74078

Received March 4, 1999

Three heteroarotinoids containing a nitrogen atom in the first ring and a C−O linking group between the two aryl rings were synthesized and evaluated for RAR and RXR retinoid receptor transactivation, tumor cell growth inhibition, and transglutaminase (TGase) induction. Ethyl 4-(*N*,4,4-trimethyl-1,2,3,4-tetrahydroquinolinyl)benzoate (**1**) contained an N-CH_3 group and activated all retinoid receptors except for RARγ. Inceasing the hydrophobicity around the rings with analogues ethyl 4-(*N*,4,4,7-tetramethyl-1,2,3,4-tetrahydroquinolin-6-oyloxy)benzoate (**2**) [7-methyl group added] and ethyl 4-(4,4-dimethyl-*N*-isopropyl-1,2,3,4-tetrahydroquinolin-6-oyloxy)benzoate (**3**) [NCH$(CH_3)_2$ group at C-4] increased the potency and specificity for RARα, RARβ, and RXRα, compared to **1**, but had little effect on RXRβ and RXRγ activation. Although **1** and **3** were unable to activate RARγ, **2** did activate this receptor with efficacy and high potency equal to that of 9-*cis*-retinoic acid (9-*c*-RA). All three heteroarotinoids exhibited 5−8-fold greater specificities for RARβ over RARα. In addition, esters **1**−**3** inhibited the growth of two cell lines each derived from cervix, vulvar, ovarian, and head/neck tumors with similar efficiencies to that of 9-*c*-RA through a mechanism independent of apoptosis. The vulvar cell lines were the most sensitive, and the ovarian lines were the least sensitive. Ester **2** was similar to **1** and **3** except that **2** was a much more potent growth inhibitor of the two vulvar cell lines, which is consistent with strong RARγ activation by **2** (but not by **1** and **3**) and the high levels of RARγ expression in skin. All three heteroarotinoids induced production of TGase, a marker of retinoid activity in human erythroleukemic cells. Esters **2** and **3** were the more potent TGase activators than **1**, in agreement with the stronger activation of the RAR receptors by **2** and **3**. The biological activities of these agents, and the RARγ potency of **2** in particular, demonstrate the promise of these compounds as pharmaceutics for cancer and skin disorders.

Introduction

Retinoids are analogues of vitamin A with promise as pharmaceuticals for cancer and other diseases, but there are limitations due to toxicity even for the endogenous *trans*-retinoic acid (*t*-RA), 9-*cis*-retinoic acid (9-*c*-RA), and 13-*cis*-retinoic acid (13-*c*-RA).[1] Therapeutic potential of structurally related stilbene-like analogues, such as TTNPB, is compromised by a maximum tolerated dose (MTD) which is 1000-fold smaller compared to that of *t*-RA, a metabolite of vitamin A.[2,3] It has been shown that the insertion of an oxygen atom into the partially saturated ring in TTNPB decreased the toxicity to an MTD equal to that of *t*-RA.[3] However, the biological activity of the oxygen-containing heteroarotinoid was only 31% as efficacious in transactivating a retinoic acid response element (RARE) as compared to *t*-RA.[3] Heteroarotinoids (structurally related to the clinical Etretinate)[1] containing a sulfur or nitrogen atom appear to exhibit significantly higher biological activity than the oxygen-containing counterparts.[3] In an effort to enhance useful activity in the heteroarotinoid system, the nitrogen-containing compounds **1**−**3** were obtained and evaluated with respect to biological activity and receptor specificity. These systems possess 2-atom link-

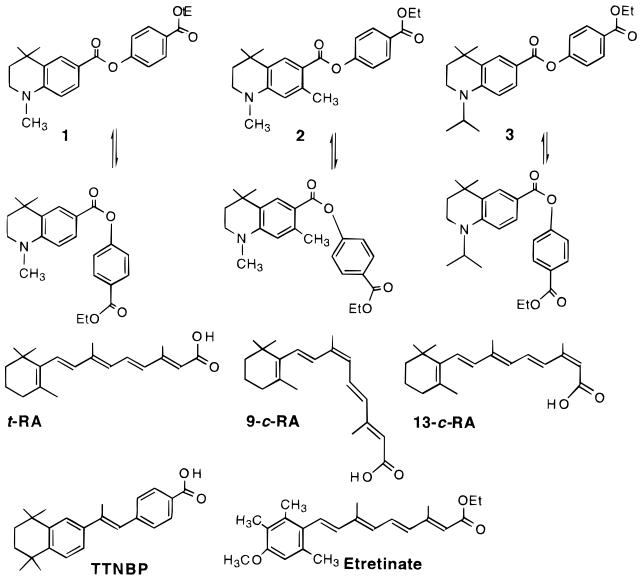

* Corresponding authors. For biology: e-mail, Doris-Benbrook@OUHSC.edu. For chemistry and modeling: e-mail, kdberlin@bmb-fs1.biochem.okstate.edu.
[†] Department of Obstetrics & Gynecology.
[‡] Department of Chemistry.
[§] Department of Urology.
[▽] Department of Otorhinolaryngology.
[⊥] Department of Biochemistry & Molecular Biology, OUHSC.
[||] Department of Biochemistry & Molecular Biology, OSU.

10.1021/jm9900974 CCC: $18.00
Published on Web 08/19/1999

Scheme 1. Synthesis of **2**

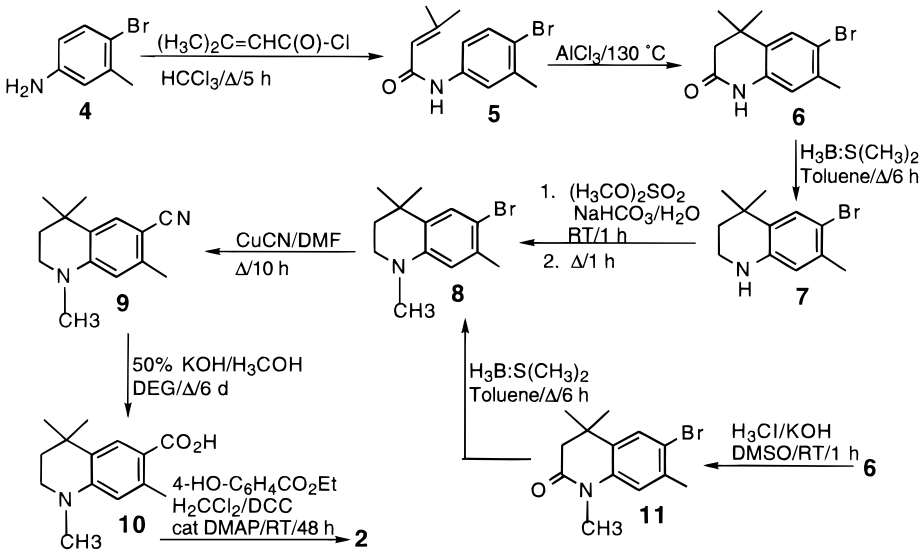

ers (C−O) between the two rings, a bonding situation which increases the flexibility of the heteroarotinoids and increases biological activity in comparison with analogues containing alkenyl linkers.[3]

Retinoids act through two classes of nuclear receptors, RARs and RXRs, each of which contain subtypes classified as α, *β*, and *γ*. The arotinoid TTNPB, like *t*-RA, activates the RARs but not the RXRs. Substitution of a hydrogen atom by a methyl group at C-3 (position equivalent to C-7 in the heteroarotinoids) of TTNPB confers RXR activation capability to the molecule.[4,5] The RXR selectivity of the 3-methylated stilbene analogues may result from the change in energy barrier for rotation by the aryl rings around the linker group, thus generating a slight change in the average conformation of the entire system. In this work we report the effect of the corresponding methyl group at C-7 on the receptor activation profile of heteroarotinoid **2**. Expectedly, the presence of such a hindering methyl group will decrease the flexibility around the C−O linker and alter receptor specificity.

The presence of a lipophilic group at C-4 extending outward and away from the plane of the ring appears to be necessary for maximum activation of RAR receptors.[6] Substitution of an oxygen atom for C-4 resulted in weak binding[3] to the RAR receptors, while substitution with a methyl, isopropyl, or sulfur moiety at the same position might cause strong binding to RAR receptors.[3,7] Therefore, more effective screening of a nitrogen atom at the same position by a nonpolar isopropyl group, such as in **3**, was reasoned to result in reduced polarity exposed from this position and improved hydrophobic bonding to the receptor.

In this report, three nitrogen-containing heteroarotinoids were evaluated for anticancer activity against cell lines derived from leukemia and solid tumors. Leukemia is currently being treated with *t*-RA which causes remission of acute promyelocite leukemia (APL) by inducing differentiation and retarding growth of APL cells.[8] It has been found that treating some human erthyroleukemia (HEL) cells with *t*-RA results in cell differentiation accompanied by a 9-fold increase in tissue transglutaminase (TGase) activity.[9] TGases are Ca^{2+}-dependent enzymes which catalyze posttranscriptional modifications of proteins by introducing intermolecular ϵ-(γ-glutamyl)lysine isopeptide bonds.[10,11] Recently, it was observed that certain nitrogen- and sulfur-containing heteroarotinoids also induced TGase production in HEL cells and, in fact, exerted greater induction than some oxygen-containing analogues.[3]

The effectiveness of the three nitrogen-containing heteroarotinoids described herein against solid tumors was assessed by determining their abilities to inhibit growth and induce a natural form of cell death (called apoptosis) in each of the two cell lines derived from cervical, vulvar, ovarian, and head and neck tumors. The size of the tumor depends on the rate of growth versus apoptosis in its cell population. Retinoids have the potential to cause tumor shrinkage by inhibiting growth and inducing apoptosis. Some retinoids are good growth inhibitors and poor inducers of apoptosis, while others are poor growth inhibitors but potent inducers of apoptosis.[12] Both types of retinoids have the potential to shrink tumors by altering the balance between growth and apoptosis.[11]

Chemistry

The synthesis of **1** was described previously.[3] Syntheses for compounds **2** and **3** are outlined in Schemes 1 and 2, respectively. A major modification in Scheme 2 as shown for conversions **4** → **5** → **6** → **7** → **8** → **9** → **10** → **2** resulted when direct lithiation of **8** failed, and an alternative approach was required to eventually produce acid **10**. *N*-Acylation of **4** (Scheme 1), followed by ring closure of **5** via a solid-phase reaction with $AlCl_3$, gave lactam **6**. Reduction of **6** to amine **7** was facile although the purification of **7** required chromatography. *N*-Methylation of **7** was modestly successful and generated low-melting **8**. An improved procedure to obtain **8** was also realized by first converting lactam **6** to the *N*-methyl analogue **11** which was more readily reduced to **8**. This proved the structure of **8**. Replacement of the bromine atom in **8** by a nitrile group was achieved using CuCN/DMF as shown and gave **9** in high yield. Hydrolysis of **9** to acid **10** required several days, and the yield was modest (38%). Esterification of **10** occurred

Scheme 2. Synthesis of **3**

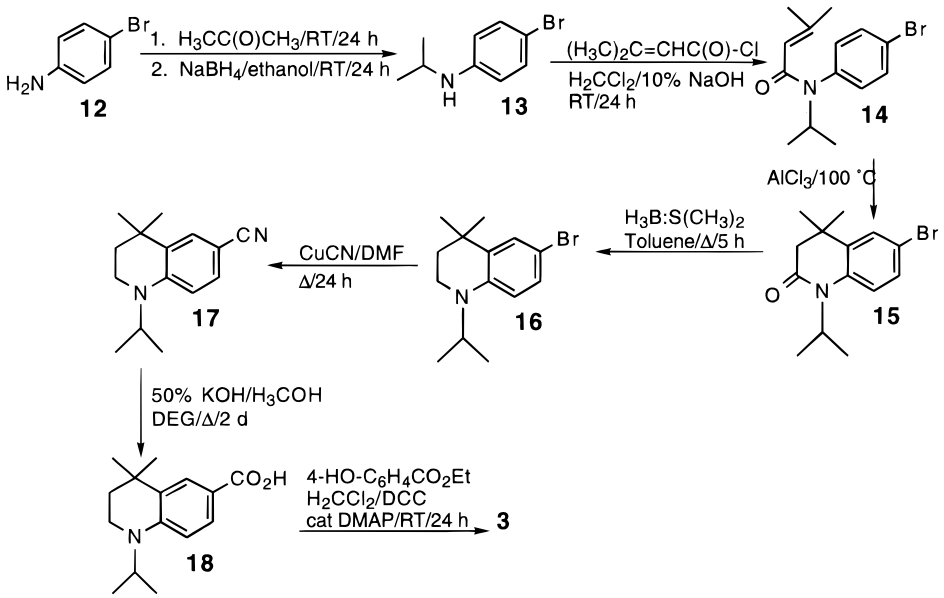

Table 1. Potency (EC_{50}, nM) and Efficacy (% of 9-*c*-RA) of Retinoid Receptor Transactivation and TGase Induction by the Three Nitrogen-Containing Heteroarotinoids **1**−**3**

	RAR			RXR			
heteroarotinoid	α	β	γ	α	β	γ	TGase induction
1 EC_{50}[a]	1128	256	NA	601	33	20	ND
% eff[b]	45	64	0	47	53	52	37
2 EC_{50}[a]	796	92	6	102	70	49	ND
% eff[b]	64	63	103	53	55	52	49
3 EC_{50}[a]	217	41	NA	12	47	27	ND
% eff[b]	59	71	0	62	45	47	49

[a] The potency is the concentration of the agent that induces half of the agent's maximal activity (not relative to 9-*c*-RA). [b] The efficacy was derived by dividing the maximal activity of the heteroarotinoid by the maximal activity of 9-*c*-RA for the receptor transactivation assay and by the maximal activity of *t*-RA for the TGase assay. The maximal activity occurred at the maximal concentration used (10 μM) for all three heteroarotinoids and for both assays. ND, not done; NA, not active.

by the usual method, but again the conversion was apparently hindered by the 7-methyl group which in turn reduced the yield of ester **2**.

Heteroarotinoid **3** was obtained as described in Scheme 2. The sequence of reactions involving **12** → **13** → **14** → **15** → **16** → **17** → **18** → **3** paralleled to some degree that shown in Scheme 1 for **2**. The conversion of bromide **16** to the nitrile **17** was much more facile than the counterpart in Scheme 1, apparently due to the absence of the C-7 methyl group in **16**.

The rationale for the comparison of **1** and **2** was based on the premise that a decrease in flexibility around the C−O bond due to the presence of the 7-methyl group, as in **2**, would alter the RAR receptor binding capability of the molecule and therefore the activity of the ligand−receptor complex formed. More effective screening of the nitrogen atom by an isopropyl group, as in **3**, was reasoned to reduce the polarity at this position for improved hydrophobic bonding in the receptor for RARs as activated by *t*-RA. TTNBP, an arotinoid with strong anticancer activity, is also nonpolar at C-1 and C-4, for example. Etretinate, a clinically used retinoid,[1] is also rather nonpolar at the ring end of the molecule as is true for **1**−**3**.

Biology

The biological activities of **1**−**3** were assessed at the molecular level for activation of nuclear receptors and at the cellular level for inhibition of tumor cell growth and induction of TGase activity in HEL cells. The standards used for comparison purposes was 9-*c*-RA and TTNPB.

To evaluate the receptor activation, CV-1 cells were cotransfected with the specific retinoic acid receptor expression constructs and the βRARE-*tk*-CAT reporter plasmid which has been shown to be activated by both RAR/RXR heterodimers and RXR/RXR homodimers.[13] Structural variations in **1**−**3** had distinct effects on receptor-dependent transactivation as illustrated in Table 1. Ester **1** transactivated the RARE through RARα and RARβ but not through RARγ. The activation of all three RXR receptors by this compound was not entirely surprising since prior heteroarotinoids had confirmed RXR activation capacity.[3]

Substitution of hydrogen by a methyl group at the 7-position significantly increased RARγ efficacy for **2** but had minimal effects on RARα and RARβ efficacies as compared to that noted in **1** and **3**. Although RXRβ and RXRγ were only slightly altered by the presence of the 7-methyl group in **2**, RXRα potency was markedly increased in comparison to **1**. The latter is consistent with the effects of this same substitution on TTNPB.[3] The presence of the *N*-isopropyl group in **3** also increased RARα, RARβ, and RXRα potencies compared to **1**, while exerting minimal effects on RARγ, RXRβ, and RXRγ activation. Thus, the most striking effect of

the 7-methyl substitution in **2** was conference of RARγ activation with a potency and efficacy equal to that of 9-*c*-RA. All three compounds exhibited nearly equal or greater specificity for RARβ over RARα.

Heteroarotinoids **1**−**3** were appraised for ability to induce TGase (Table 1), a marker of retinoid efficacy in leukemia cells.[3] In agreement with the strong activation of the retinoid receptors, **2** and **3** exerted a 49% induction of TGase activity in HEL cells in comparison to the 37% induction by **1**. Treatment of HEL cells with 10 μM *t*-RA increased cellular differentiation, inhibited cell proliferation, and increased tissue TGase.[9−11] Biological effects were observed at retinoid concentrations of 10 μM, and cell viability was greater then 90% in HEL cultures with *t*-RA or the heteroarotinoids.[9]

Compounds **1**−**3** were screened for ability to inhibit growth on a panel of two cell lines each derived from cervix, vulva, ovary, and head and neck tumors (Figure 1). The vulvar cells were the most sensitive, and the ovarian cells were the least sensitive to retinoid treatment. In a majority of cases, the heteroarotinoids were similar in efficacy to 9-*c*-RA. The efficacy for individual compounds varied depending upon the cell line. The most dramatic growth inhibition was exerted by **2** on the two vulvar carcinoma cell lines, consistent with the potent RARγ specificity of this compound and with the fact that the retinoid effects in keratinizing skin, such as vulva, are mediated mainly through the high levels of RARγ expressed in this type of epithelium.[14,15]

The greater than 75% growth inhibition observed for **2** with the vulvar cell line indicates that cell loss might be occurring due to apoptosis or necrosis. It is more likely, however, that the mechanism in this experiment is due to a slowing down of the cell cycle because there were more cells present at the end of the 3-day treatment period than at the initiation. This high degree of growth inhibition without cell loss is possible for the vulvar cell lines because such cells exhibited a rapid growth rate with a doubling time of 30 h. Therefore, at the end of 72 h of treatment in the experiment, the control cultures had increased in cell number by approximately 4.5 times (12 000 cells). The cultures treated with **2** contained approximately 25% of the cells present in the control culture (3 000 cells) which is greater than the 2 000 cells plated *before* the initiation of treatment.

To determine if induction of apoptosis was part of the mechanism by which nitrogen-containing heteroarotinoids decrease tumor cell culture density, the effects of **2** and **3** were elevated on the most sensitive cell line, namely SW962 (Figure 2). Agent 4HPR was used as a positive control for retinoid induction of apoptosis, and *t*-RA was used as a control for retinoid growth inhibition in the absence of apoptosis.[12] The apoptotic cells in these cultures were quantitated using an ELISA assay for enrichment of mono- and oligonucleosomes that result from fragmentation of chromosomes by endogenous nucleases during apoptosis. As expected in the treated cells, 4HPR enriched apoptosis by more than 5-fold, while **2**, **3**, and *t*-RA had little effect. This observation classifies these nitrogen-containing heteroarotinoids as members of the nonapoptotic retinoid group along with *t*-RA.

Molecular Modeling. The utility of molecular modeling in attempts to determine ligand−receptor interactions has not been documented with heteroarotinoids to any appreciable extent. The availability of data from the X-ray analysis of RARγ[16] and RXRα[17] was an

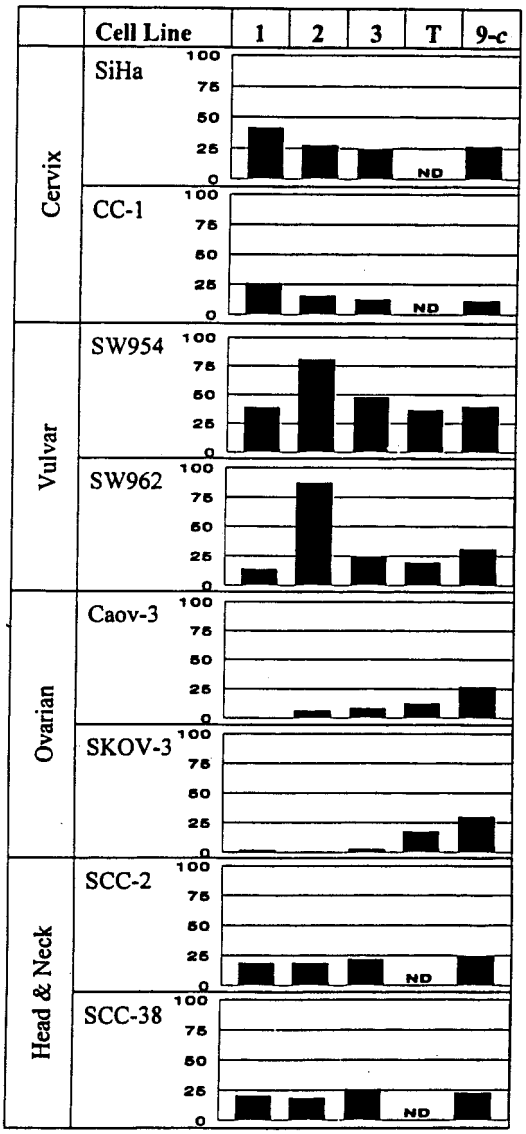

Figure 1. Data from the percent of growth inhibition of certain cells lines by **1**−**3**, TTNPB, and 9-*c*-RA. Such cells from various carcinoma cell lines were plated in microtiter plates and treated with 10 μM of agents **1**−**3** or with TTNPB (T) or 9-*c*-RA (9-*c*) for 72 h. The concentration of cells at the end of 3 days was determined by SRB assay. Growth inhibition was measured as the percent of cell loss in the treated cultures relative to control cultures treated with solvent (DMSO).

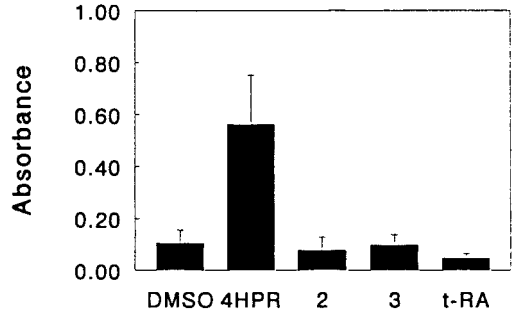

Figure 2. Comparison of apoptosis in SW962 cells treated with various retinoids or solvent. The absorbance indicates the presence of mono- and oligonucleosomes in the cyctoplasm, which is characteristic of apoptotic cells.

Table 2. Energies of Interaction of Flexible Ligand−Fixed RARγ (kcal/mol)[a]

ligand		run1	run2	run3	run4	run5
	seed_num	5000	8000	13000	18000	23000
	gen_num	25000	20000	15000	30000	10000
	meth_sco	roul	roul	tour	roul	roul
t-RA	sol_num	20	20	20	15	20
	int_ener	−64.67	−58.29	−34.71	−75.73	−33.56
	% conv	40	35	16	44	7
9-*c*-RA	sol_num	10	12	16	3	20
	int_ener	−15.48	−9.321	−7.439	−17.33	−5.38
	% conv	60	47	12	82	9
1	sol_num	6	12	12	2	14
	int_ener	8.351	12.583	21.486	5.371	22.98
	% conv	61	40	15	74	11
2	sol_num	8	8	10	7	15
	int_ener	2.473	3.618	21.486	5.371	22.98
	% conv	40	33	21	78	3
3	sol_num	18	20	20	20	20
	int_ener	−37.52	−30.63	−29.51	−45.29	−25.6
	% conv	40	24	14	53	0.0

[a] Seed_num, seed number; gen_num, generation number; meth_sco, method of scoring; sol_num, solution number; int_ener, interaction energy; % conv, percent convergence; roul, roulette method of scoring; tour, tournament method of scoring.

incentive to examine **1**−**3**, *t*-RA, and 9-*c*-RA as ligands for the rigid form of RARγ, as exemplified by the docking site in RARγ with *t*-RA as the ligand in the X-ray structure. In addition, more flexible forms of both the receptor and the ligands were evaluated in terms of the lowest energy conformations for both ligand and receptor. The crystallographic structure of the crystallized RARγ−ligand (*t*-RA) system was obtained from the Protein Data Bank (see Experimental Section). The binding pocket of the RARγ was defined with the following amino acid residues: Phe201, Trp227, Phe230, Ser231, Leu233, Ala234, Lys236, Cys237, Ile238, Leu268, Leu271, Met272, Arg274, Ile275, Arg278, Phe288, Ser289, Gly303, Phe304, Pro306, Leu307, Gly393, Ala394, Arg396, Ala397, Leu400, Met408, Ile412, and Met415 with a radius of 10 Å around these amino acids.[18]

The calculations were performed using SYBYL 6.5 and employing the licensed "Biopolymer" which possesses a program designated "FlexiDock". The FlexiDock, SYBYL 6.5 release, was used for docking all ligands into the binding pocket of RARγ. The parameters for the genetic logarithm of FlexiDock were used as set in default by the manufacturer with the exception of using Tournament instead of Roullete Wheel as a scoring method in one round of calculations for each ligand. For comparison purposes, the *t*-RA in the binding site of the crystallogaphic structure of RARγ containing the crystallographic structure of *t*-RA was removed, and independently *t*-RA was inserted and docked as a check on the validity of the technique. For this superimposition an rmsd value of 0.3464 (SD = 0.1362) was obtained which lends credibility to the methodology. The energy of interaction between the crystal structure of *t*-RA in the RARγ binding pocket was calculated to be −73.592 kcal/mol with the crystal structure conformational energy of *t*-RA at 64.243 kcal/mol. Taking the crystal structure of RARγ and docking *t*-RA gave an energy of interaction of −75.728 kcal/mol and a conformational energy for *t*-RA of 23.872 kcal/mol.

All ligands were drawn with carboxylate anions using the fragment library of Insight Discover 97. The Gasteiger−Huckel method was employed using SYBYL 6.5 for the charge assignment of each ligand, with formal charges of −0.5 assigned to each oxygen atom of the carboxylate group resulting in a total charge of −1.0 for all ligands. The energy minimization of ligands was accomplished with SYBYL 6.5 using Tripos force field with the Powell method of line direction search. Charges were computed before each minimization and used as "current" in the energy setup option box. The rmsd was set to 0.001, and the gradient was set to 0.005 kcal/mol Å. The conformational search was done with 9-*c*-RA using simulated annealing where the molecule was allowed to anneal at 300 K. More than 100 conformations of 9-*c*-RA were evaluated from this process, and one conformer was selected which most closely resembled the normal conformation of *t*-RA. The conformational energy difference between the normal 9-*c*-RA and that conformer which most closely mimics *t*-RA in general appearance was 0.87 kcal/mol.

Discussion

Results reported herein demonstrate that specific substitutions on the heteroarotinoid structure significantly alter the biological activity of the agents. For example, modifications of structures **2** and **3**, compared to heteroarotinoid **1**, resulted in increased receptor activation with varying effects on growth inhibition, depending upon the cell line. The variability in the responses of the different cell lines represent the complexity of the retinoid response pathway. Retinoids have been shown to regulate not only gene expression but also growth factor expression and the activities of several protein kinases.[19−21] Therefore, the response of a cell line to retinoid treatment depends on the expression patterns of retinoid receptors and certain cofactors, growth factor receptors, kinases, and phosphatases. The addition of the 7-methyl group in **2** conferred RARγ activation on a structure otherwise devoid of this type of activity as in **1**. The increased susceptibility of the vulvar cell lines to agent **2**, in comparison to the other epithelial carcinomas, can be explained by the higher levels of RARγ expression in skin over other epithelial types.[22] This observation is consistent with the RARγ mediation of retinoid pharmacological action in skin.[14,15] The EC_{50} value of 6 nM and the 103% efficacy of **2** (Table 2), in comparison to that of 9-*c*-RA, indicate that **2** may be useful as a pharmaceutical agent for disorders of the skin.

Table 3. Energies of Interaction of Flexible Ligand−Flexible RARγ (kcal/mol)[a]

ligand		run1	run2
	seed_num	18000	23000
	gen_num	30000	10000
	meth_sco	roul	roul
t-RA	sol_num	20	20
	int_ener	−40.34	−23.56
	% conv	60	33
9-*c*-RA	sol_num	12	20
	int_ener	−20.358	− 9.756
	% conv	65	9
1	sol_num	20	20
	int_ener	−57.008	−46.406
	% conv	88	7
2	sol_num	20	20
	int_ener	−22.799	−17.94
	% conv	80	15
3	sol_num	20	20
	int_ener	−78.18	−75.53
	% conv	85	40

[a] Seed_num, seed number; gen_num, generation number; meth_sco, method of scoring; sol_num, solution number; int_ener, interaction energy; % conv, percent convergence; roul, roulette method of scoring.

TGase induction in human myeloid leukemic cells is mediated through a pathway involving RARs.[23] On the other hand, TGase induction in rat tracheobronchial epithelial cells is mediated through a pathway involving RXRα.[14] These results may not be considered conflicting since nuclear receptors function in cooperation as dimers.[24] While the RXRs can function both as homodimers (RXR/RXR) and as heterodimers with RARs (RAR/RXR), the RARs function only as heterodimers (RAR/RXR). In agreement with this fact, myeloid cells are induced to differentiate by a retinoid which selectively activates RAR/RXR heterodimers, but not by a retinoid which selectively activates RXR/RXR homodimers.[25] Therefore, if the major mediator of retinoid effects on TGase induction is the RAR/RXR heterodimer, then 9-*c*-RA, which activates both partners, would be expected to exhibit greater activity than *t*-RA, which activates only RARs. The more potent TGase induction by **2** and **3**, in comparison to that by **1**, is consistent with the greater receptor activation by **2** and **3**. The nearly equal efficacies of **2** and **3** on TGase induction, despite the strong activation of RARγ by **2** but not by **3**, suggest that RARγ either is not required or is redundant in TGase induction of HEL cells. In conclusion, the potency of the nitrogen-containing heteroarotinoids **1**−**3** in receptor activation, tumor cell growth inhibition, and TGase induction warrants toxicity testing as the next step prior to clinical trials.

Illustrations from the modeling work are shown in Figures 3 and 4. The docking experiments with **1**−**3** using parameters obtained from X-ray data (devoid of the 119 water molecules) for the rigid RARγ system[16] did not indicate a good correlation with the activity observed. In addition, docking experiments with the 119 water molecules present in the rigid RARγ system did not result in significant conformational changes in any of the ligands or with the energy of interaction with the exception of small differences in electrostatic energies. Therefore, the following discussion is primarily based upon results with a *flexible* RARγ system devoid of water.

Although agent **2** displayed strong RARγ activation, **2** did not dock rigid RARγ with an interaction energy better than that of **3** or 9-*c*-RA. Possible explanations for this is that the crystal structure may not reflect the active form of RARγ−ligand or that some of the conformations of the amino acids in the binding domain are not so important for selectivity and activity of RARγ. Changing the rigid RARγ−ligand system to a flexible RARγ system, via an option in the FlexiDock program, and then docking *t*-RA as a flexible ligand in the flexible RARγ molecule gave a flexible RARγ−ligand molecule with a conformation of RARγ which differed only slightly from that in the crystal structure of RARγ−ligand. The flexible RARγ system in our work refers to the binding domain in which all amino acids have freedom to move in all dimensions. An interaction energy of −40.34 kcal/mol was noted for the flexible RARγ−flexible ligand. This is strong indication of the high stability of the complex. Superimposition of this flexible−flexible system on the rigid RARγ−ligand system produced an rmsd of 0.01 with respect to the majority of amino acids. Some deviations from this rmsd value were noted with certain amino acids, namely Phe201 (0.1931), Lys236 (0.752), Cys237 (0.420), Arg278 (0.185), Ser289 (0.523), Leu400 (0.128), Ile412 (0.236), and Met415 (0.121).

As further support for the contention that not all of the amino acids in the region of the binding pocket are responsbile for activation → binding, the flexible RARγ−*t*-RA system was made "fixed" and the *t*-RA was removed while agents **1**−**3** were then docked in succession as flexible ligands. No improvement was observed in the interaction energies (data not included). In contrast, using the flexible RARγ−flexible ligand model resulted in all ligands docking favorably with favorable negative interaction energies for ligand and receptor. Figure 3 illustrates the various docking experiments performed with flexible RARγ. For comparison purposes, **A** (Figure 3) shows the binding pocket with amino acids of rigid RARγ based on crystallographic data. Docking flexible *t*-RA, 9-*c*-RA, **1**, **2**, and **3** with flexible RARγ led to the various flexible ligand-bound RARγ systems **B**−**F**, respectively (Figure 3). Extraction of the ligands from **B**−**F** exposed the individual binding pockets (not shown), and superimposition of the binding pocket of *t*-RA on those binding pockets for 9-*c*-RA and **1**−**3** gave images **G**−**J**, respectively, as described in Figure 4. Small conformational differences in the binding pocket of RARγ were observed after docking *t*-RA, both receptor and ligand being in the flexible modes, as compared to the resulting conformations observed when **1**−**3** were docked. The flexible RARγ-ligand flexible 9-*c*-RA (annealed) matched well with **B** to give the dual images in **G**. Likewise, agent **2** system matched well (**I**) with the exposed flexible RARγ devoid of *t*-RA. In contrast **1** (**H**) and **3** (**J**) clearly possess major deviations in terms of interactions of these ligands with the amino acids in the docking pocket of flexible RARγ. With **2**, only deviations greater than a rmsd value of 0.001 were noted, such as with certain amino acids as Phe201 (0.397), Leu233 (0.805), Lys236 (1.192), Cys237 (0.42), Ile275 (0.185), Arg278 (0.595), Ser289 (0.339), Phe304 (0.134), and Met408 (0.478). Differences in the amino acid residues using 9-*c*-RA as the flexible ligand were Phe231

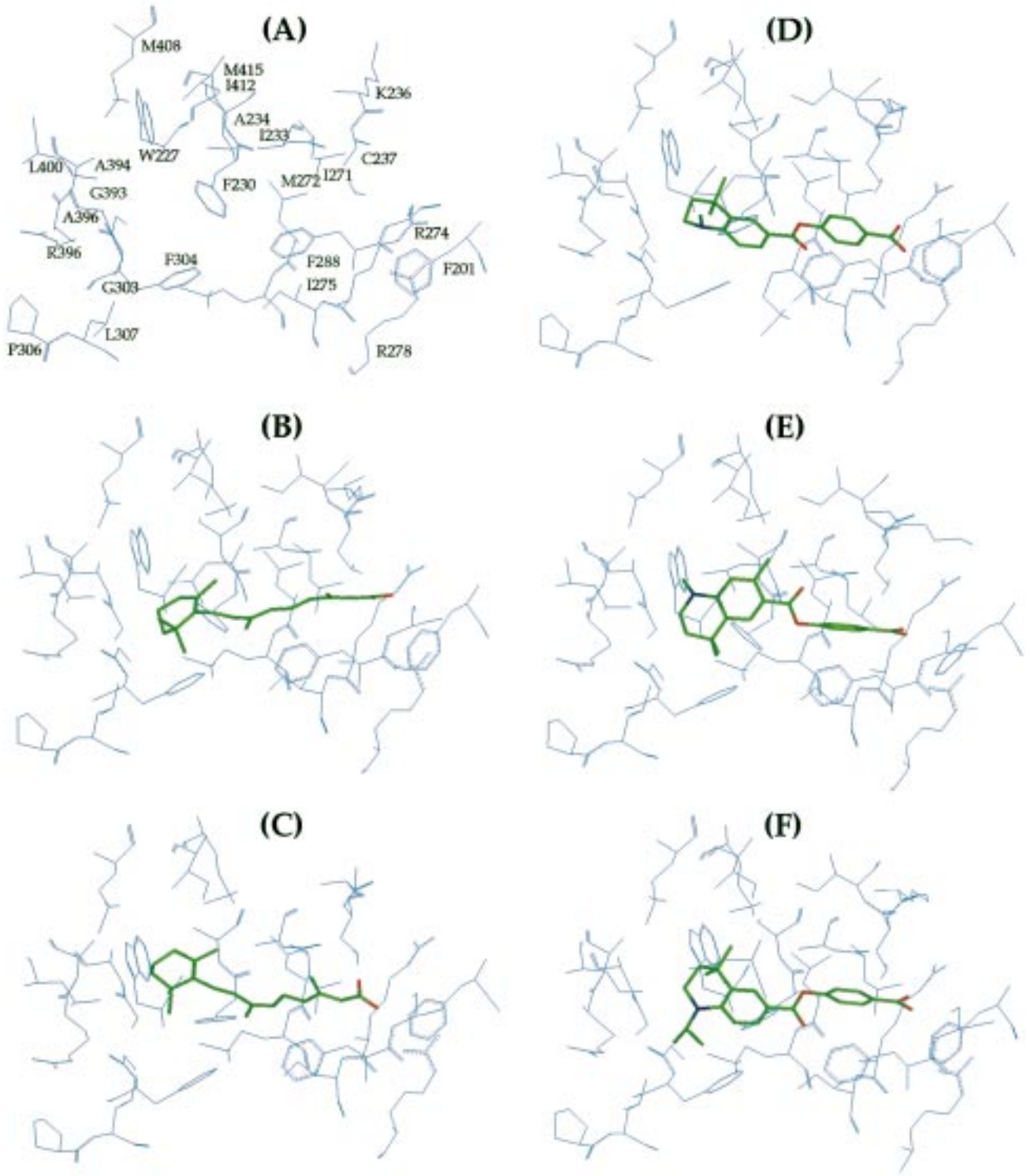

Figure 3. RARγ with bound ligands. A, Binding pocket with the amino acids listed of RARγ from X-ray diffraction data with *t*-RA extracted. B, Binding pocket of flexible RARγ bound with flexible *t*-RA. C, Binding pocket of flexible RARγ bound with flexible 9-*c*-RA. D, Binding pocket of flexible RARγ bound with flexible **1**. E, binding pocket of flexible RARγ bound with flexible **2**. F, Binding pocket of flexible RARγ bound with flexible **3**.

(0.202), Lys236 (0.698), Phe230 (0.501), Ser231 (0.415), Ser289 (0.378), Phe304 (0.143), Leu307 (0.263), Arg396 (0.151), Ile412 (0.462), and Ile275 (0.435). The larger number of amino acid residues involved with larger deviations in orientations observed with docked **1** and **3** is in agreement with both agents being RARγ inactive. Superimposition of the ligand binding domains of RARγ, each with the previously cited low-energy conformer of 9-*c*-RA and *t*-RA removed, had a total rmsd = 0.22.

Cross-checking the superimposition results with visual inspection of the final conformations of RARγ and ligands leads to the speculation that amino acids Phe230, Met272, Leu271, and Ala234 are the most important for RARγ activation which agrees with previous suggestions.[16] The phenyl ring of Phe230 assumes a different orientation with respect to the remaining amino acid residues and with regard to inactive ligands as compared to active *t*-RA and **2**, for example (Figure

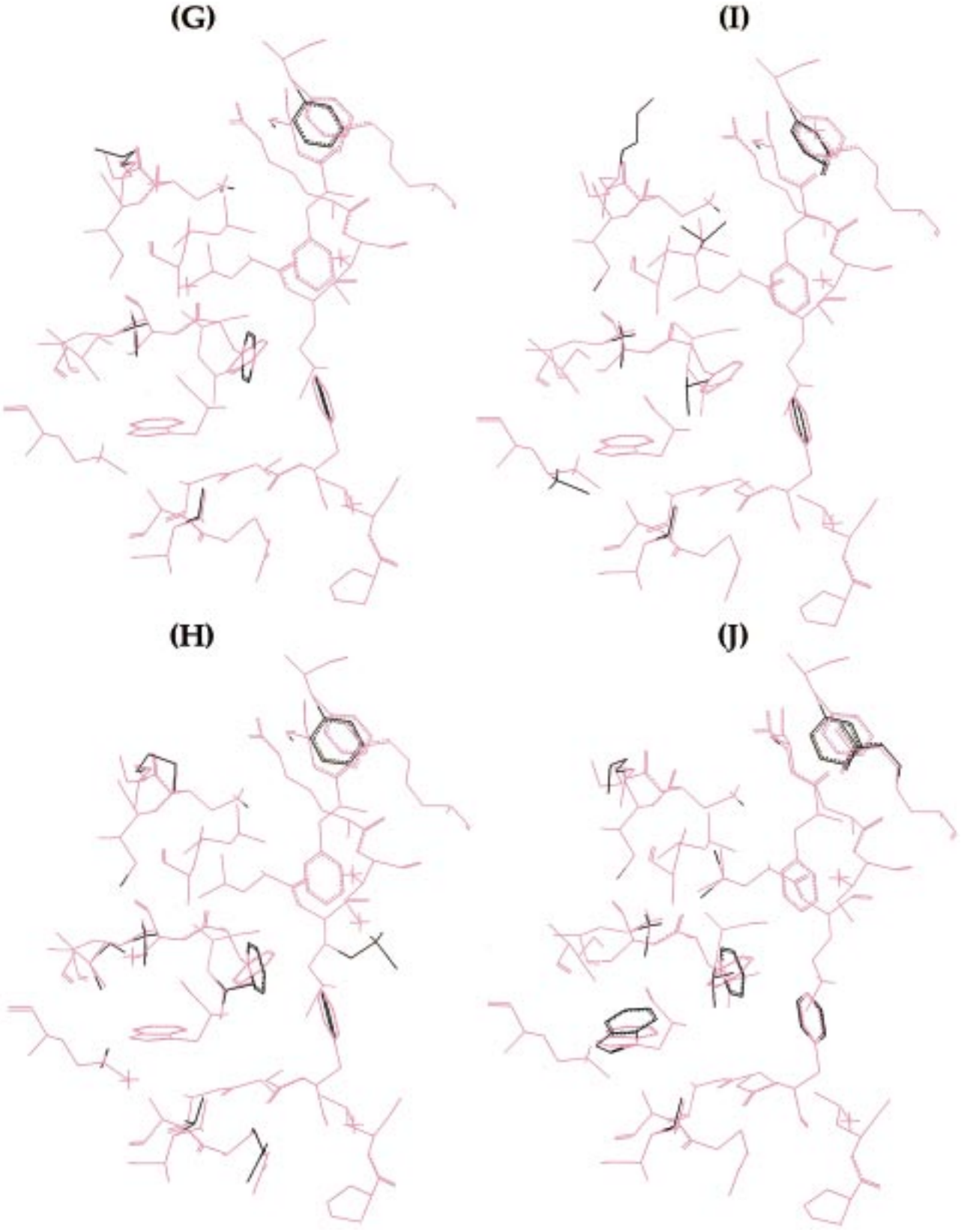

Figure 4. Binding pocket of flexible RARγ with *t*-RA removed and superimposed upon the binding pockets of RARγ with the ligands 9-*c*-RA, **1**, **2**, and **3** removed. G, Superimpositions of the binding pocket of B (magenta) upon the binding pocket of C (black) both devoid of the ligands *t*-RA and *9-c*-RA, respectively. The conformations of the following amino acids from the two pockets did **not** match with respect to Lys236, Phe201, Phe230, Ser231, and Ala394 with minor deviations in Leu271 and Ile412. H, Superimpositions of the binding pocket of B (magenta) upon the binding pocket of D (black) both devoid of the ligands *t*-RA and **1**, respectively. The conformations of the following amino acids from the two pockets did **not** match with respect to Lys236, Phe201, Phe230, and Arg396 with minor deviations in Ala234, Phe304, Ile412, and Met415. I, Superimpositions of the binding pocket of B (magenta) upon the binding pocket of E (black) both devoid of the ligands *t*-RA and **2**, respectively. The conformations of the following amino acids from the two pockets did **not** match with respect to Lys236 with minor deviations in Met408, Ile412, Ser231, Leu271, Ile412, and Phe304. J**,** Superimpositions of the binding pocket of B (magenta) upon the binding pocket of F (black) both devoid of the ligands *t*-RA and **3**, respectively. The conformations of the following amino acids from the two pockets did **not** match with respect to Phe201, Phe230, and Trp227 with minor deviations in Ala394, Ile412, Ala234, Arg278, and Lys236.

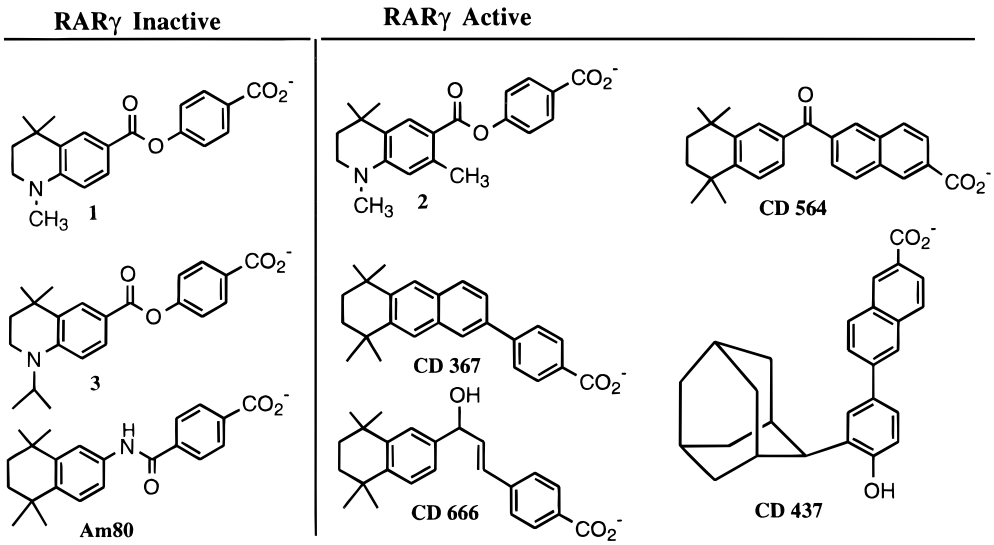

Figure 5. Listing of RARγ active and RARγ inactive structures as related to **1**−**3**.

4). Possibly Phe230 acts as a "switch" for activation by assuming different orientations with specific ligands. With 9-*c*-RA, the phenyl ring of Phe230 lies in a position somewhat between that found with *t*-RA and **2** (which match well) as compared to the position observed in inactive **1** and **3**.

The role of Ala234, Met272, and Leu271 would appear to be in the selectivity of the ligand for RARγ through a series of van der Waal interactions with part of the ligand. Since **2** differs from **1** by only the methyl group at the 7-position, the additional nonpolar methyl group may interact with hydrophobic regions of Ala234, Leu271, and Met272. Such interaction may be responsible for positioning the ligand in the binding cavity in such a manner that the hydrophobic region of **2** is identical or quite similar in position and interaction experienced by the hydrophobic region in the binding of *t*-RA to RARγ. With **1** and **3**, this interaction does not occur with Ala234 and Leu271, and the ligands are free to reposition themselves in the cavity. The end result is that the ligands interact with the receptor in what appears to be a favorable arrangement, but the phenyl ring of Phe230 is rotated approximately 120°. Perhaps because of this new orientation additional changes occur within and on the surface of the receptor making the receptor incapable of binding to transcription cofactors. As a defense for this reasoning, attempts were made to dock the retinoids shown in Figure 5 with our model flexible RARγ. All ligands which were reported as RARγ active docked well, and those reported[26] to be inactive did not dock well. Indeed, the position of the Phe230 matched well in systems with ligands *t*-RA, 9-*c*-RA, and **2** as well as with CD564, CD367, CD437, and CD666 but did not match well with **1**, **3**, and Am80 (Figure 5).

The very recent report[27] on the structure, via electron diffraction studies, of the solid RARγ−9-*c*-RA complex revealed that 9-*c*-RA does indeed assume a bent conformation which resembles very much the structure proposed from the modeling work described herein. Thus, it is encouraging that our modeling approach has important potential for guiding the synthesis of future modified retinoids with lower toxicity than the endogenous members. Thus, the modeling experiments appear to be instructive with respect to "turning on" RARγ for proper activation of the type initiated with *t*-RA, the endogenous ligand. Consequently, the merit of this hypothesis lies in the design and evaluation of future agents to activate RARγ for specific transcription processes, all of which await trial. It is interesting to note that certain synthetic and highly modified retinoids with an internal amide linkage, which is para to a carboxyl group on a benzene ring, have been demonstrated to induce differentiation in human promyelocytic leukemia cells (HL-60), but no references were made to RARγ activation.[28,29]

In conclusion, a decrease in flexibility around the C−O bond in **2**, due to the presence of the methyl group at the 7-position, conferred RARγ activation capacity in contrast to the parent **1**. Molecular modeling using X-ray crystallographic data of the ligand binding domain of RARγ confirmed that **2**, not **1** or **3**, interacted with the receptor in an energetically favorable fashion. The potency of the nitrogen-containing heteroarotinoids **1**−**3** in receptor activation, tumor cell growth inhibition, and TGase induction is comparable to that of 9-*c*-RA, and the decreased toxicity of the heteroarotinoid class of retinoids warrants toxicity testing of these agents as the next step prior to clinical trials.

Experimental Section

General. IR spectra were recorded on a Perkin-Elmer 2000 FT-IR as films or as KBr pellets. GC−MS data were obtained from a HP G1800A GCD System, GC electron ionization detector. FAB MS experiments were performed on a VG ZAB-2SE HRMS unit, while EI MS experiments were accomplished with an HP GC-MS ENGINE, model 5989B unit. All ^{1}H and ^{13}C NMR spectra were taken on a Varian Inova 400 MHz or a Varian XL-400 MHz BB spectrometer at 399.92 and 100.57 Hz, respectively, and signals are referenced to TMS. Melting points were determined with a Thomas-Hoover melting point apparatus and are uncorrected. Syntheses were executed, unless otherwise indicated, under an atmosphere of N_2. Elemental analyses were performed by Galbraith Laboratories, Knoxville, TN, or by Atlantic Microlab, Inc., Norcross, GA. Although the intermediates and final heteroarotinoids appeared to be relatively stable in light, precautions were taken to minimize exposure of all products to any light source as well as to the atmosphere. Pure heteroarotinoids **1**,[3] **2**, and **3** were stored in the cold and dark for indefinite periods without significant decomposition.

Ethyl 4-(*N*,4,4,7-Tetramethyl-1,2,3,4-tetrahydroquinolin-6-oyloxy)benzoate (2). To a mixture of acid **10** (0.155 g, 0.665 mmol) and ethyl 4-hydroxybenzoate (0.165 g, 0.997 mmol) were added dicyclohexylcarbodiimide (DCC; 0.274 g, 1.33 mmol) and DMAP (10 mg). The resulting solution was stirred at room temperature (48 h) and then filtered. Concentration of the solution produced a heavy oil which was chromatographed over silica gel (H_2CCl_2:H_3C−OH, 100:1) to give a solid which was recrystallized (hexane:EtOAc, 4:1) to yield white crystals of **2** (0.065 g, 24%): mp 69−71 °C; IR (KBr) 1718 cm^{-1}; ^1H NMR ($DCCl_3$) δ 1.31 (s, 6 H, 2 CH_3), 1.40 (t, 3 H, CH_2CH_3), 1.74 (t, 2 H, J = 6.0 Hz, CCH_2), 2.60 (s, 3 H, Ar−CH_3), 3.00 (s, 3 H, NCH_3), 3.36 (t, 2 H, J = 6.0 Hz, CH_2N), 4.39 (q, 2 H, CH_2CH_3), 6.38 (s, 1 H, Ar−H), 7.25 (d, 2 H, Ar−H), 8.09 (s, 1 H, Ar−H), 8.11 (d, 2 H, Ar−H); ^{13}C NMR ($DCCl_3$) δ 14.2 (CH_2CH_3), 22.7 (Ar−CH_3), 30.0 (Ar$C$$CH_2$), 31.5 (2 CH_3), 36.2 (Ar$C$$CH_2$), 38.8 ($NCH_3$), 47.7 ($NCH_2$), 61.2 ($OCH_2$), 112.9−155.1 (Ar−C), 165.1 (C=O), 166.0 (C=O). Anal. ($C_{23}H_{27}NO_4$) C, H, N.

Ethyl 4-(4,4-Dimethyl-*N*-isopropyl-1,2,3,4-tetrahydroquinolin-6-oyloxy)benzoate (3). To acid **17** (0.200 g, 0.810 mmol), ethyl 4-hydroxybenzoate (0.200 g, 1.2 mmol), and H_2CCl_2 (30 mL) were added DCC (∼0.500 g, 3.0 mmol) and a catalytic amount of DMAP (10 mg) with stirring. After stirring at room temperature for 24 h, the clear solution was evaporated to a heavy oil which was chromatographed (silica gel; hexane:EtOAc, 4:1) to a colorless oil. Treatment of the oil with dry hexane and chilling the mixture (0−4 °C) for 15 h induced solid formation. Filtration gave a white solid **3** (0.201 g, 63%): mp 87−89 °C; IR (KBr) 1722 cm^{-1}; ^1H NMR ($DCCl_3$) δ 1.24 (d, 6 H, J = 6.4 Hz, $CH(CH_3)_2$), 1.28 (s, 6 H, 2 CH_3), 1.38 (t, 3 H, J = 7.2 Hz, CH_2CH_3), 1.68 (t, 2 H, J = 6.0 Hz, CCH_2), 3.28 (t, 2 H, J = 6.0 Hz, CH_2N), 4.21 (m, 1 H, J = 6.4 Hz, $CH(CH_3)_2$), 4.36 (q, 2 H, J = 7.2 Hz, CH_2CH_3), 6.68 (d, 1 H, Ar−H), 7.24 (d, 2 H, Ar−H), 7.86 (dd, 1 H, Ar−H), 7.95 (d, 1 H, Ar−H), 8.04 (d, 2 H, Ar−H); ^{13}C NMR ($DCCl_3$) δ 14.3 (CH_2CH_3), 18.9 (2 CH_3), 29.5 ($CH(CH_3)_2$), 31.9 (Ar$C$$CH_2$), 35.9 ($CH_2C$), 36.8 ($CH_2N$), 47.5 ($CH(CH_3)_2$), 60.9 ($CH_2CH_3$), 109.5−155.2 (Ar−C), 165.0 (C=O), 166.0 (C=O). Anal. ($C_{24}H_{29}NO_4$) C, H, N.

***N*-(4-Bromo-3-methylphenyl)-3-methyl-2-butenamide (5)**. To the biphasic mixture of 4-bromo-3-methylaniline (**4**; 15.00 g, 0.081 mol), 10% NaOH (80 mL), and H_2CCl_2 (50 mL) was slowly (2 h) added 3,3-dimethylacryloyl chloride (11.47 g, 0.097 mol) in H_2CCl_2 (30 mL). After stirring at room temperature for 16 h, the reaction mixture was diluted with water (30 mL), and the resulting aqueous layer was extracted (H_2CCl_2, 4 × 30 mL). The combined extracts were dried (Na_2SO_4) and concentrated in vacuo to give a brown solid which was recrystallized (hexane:EtOAc, 4:1) to give **5** (14.12 g, 65%): mp 97−98 °C; IR (KBr) 3284, 1641 cm^{-1}; ^1H NMR ($DCCl_3$) δ 1.89 (s, 3 H, CH_3), 2.21 (s, 3 H, CH_3), 2.35 (s, 3 H, Ar−CH_3), 5.68 (m, 1 H, C=CH), 7.17−7.20 (m, 2 H, Ar−H), 7.41 (d, 2 H, Ar−H), 7.51 (s, 1 H, Ar−H); ^{13}C NMR ($DCCl_3$) δ 19.9 (CH_3), 22.97 (Ar−CH_3), 27.42 (CH_3), 118.25−138.4 (Ar−C), 118.2 (C=CH), 154.1 (CH_2C=C), 164.9 (C=O). MS (EI) Calcd for $C_{12}H_{12}BrNO$ ($M^{+\cdot}$): 267. Found: 267. Amide **5** was cyclized at once to lactam **6**.

6-Bromo-4,4,7-trimethyl-2-oxo-1,2,3,4-tetrahydroquinoline (6). Amide **5** (6.77 g, 0.025 mol) was heated in a standard system to 110−120 °C, and then $AlCl_3$ (5.05 g, 0.38 mol) was added portionwise over 1 h. The resulting viscous mixture was then stirred for 0.5 h at 110 °C. After cooling to room temperature, ice water was added and a brown solid formed. Chloroform (30 mL) was added, and the solid dissolved. This solution was stirred for 0.25 h, and 2 M HCl (30 mL) was added cautiously. Two layers separated, and the aqueous layer was extracted ($HCCl_3$, 5 × 30 mL). The combined organic layers were washed with aqueous 10% $NaHCO_3$ (30 mL) and brine. After drying ($MgSO_4$), the solution was concentrated to a brown solid which was recrystallized (95% ethanol) to white crystals of **6** (3.48 g, 50%): mp 179−180 °C; IR (KBr) 3209, 1686 cm^{-1}; ^1H NMR ($DCCl_3$) δ 1.31 (s, 6 H, 2 CH_3), 2.33 (s, 3 H, Ar−CH_3), 2.48 (s, 2 H, CH_2−C=O), 6.78 (s, 1 H, Ar−H), 7.40 (s, 1 H, Ar−H), 9.93 (s, 1 H, NH); ^{13}C NMR ($DCCl_3$) δ 22.3 (Ar−CH_3), 27.5 (Ar-$C$$CH_2$), 33.6 (2 CH_3), 45.0 (CH_2), 118.0−137.0 (Ar−C), 171.8 (C=O). MS (EI) Calcd for $C_{12}H_{12}BrNO$ ($M^{+\cdot}$): 267. Found: 267. Lactam **6** was converted to amine **7** immediately.

6-Bromo-4,4,7-trimethyl-1,2,3,4-tetrahydroquinoline (7). To a cooled (0 °C) solution of lactam **6** (1.0 g, 3.73 mmol) in dried, distilled toluene (20 mL) was added dropwise a solution of 10 M borane−dimethyl sulfide (0.88 g, 9.75 mmol). The mixture was stirred at 0 °C (0.25 h) and then was boiled for 6 h during which time the mixture became gray in color. After cooling to room temperature, aqueous 10% Na_2CO_3 (20 mL) was added, and the solution was stirred for 0.5 h. The organic layer separated, was dried ($MgSO_4$), and was concentrated to a light yellow oil which was chromatographed on silica gel (H_2CCl_2) to give **7** as a colorless oil (0.74 g, 78%). ^1H NMR ($DCCl_3$) δ 1.26 (s, 6 H, 2 CH_3), 1.69 (t, 2 H, J = 4.8 Hz, CCH_2), 2.30 (s, 3 H, Ar−CH_3), 3.27 (t, 2 H, J = 4.8 Hz, CH_2N), 6.35 (s, 1 H, Ar−H), 7.26 (s, 1 H, Ar−H); ^{13}C NMR ($DCCl_3$) δ 22.3 (Ar−CH_3), 30.8 (2 CH_3), 31.5 (Ar$C$$CH_3$), 36.8 ($CCH_2$), 38.3 ($CH_2N$), 47.5 ($NCH_3$), 111.4−142.6 (Ar−C). MS (EI) Calcd for $C_{12}H_{16}BrN$ ($M^{+\bullet}$): 253. Found: 253. Amine **7** was subjected to *N*-methylation directly to obtain **8**.

6-Bromo-*N*,4,4,7-tetramethyl-1,2,3,4-tetrahydroquinoline (8). A mixture of amine **7** (3.0 g, 0.01 mol), $NaHCO_3$ (1.78 g, 0.02 mol), and water (3 mL) was cooled to 15 °C and then was treated dropwise with dimethyl sulfate (1.94 g, 0.015 mol). After stirring at room temperature for 5 h, the mixture was diluted with $HCCl_3$ (25 mL) which caused a white precipitate to form. After filtration and washing ($HCCl_3$) the solid, the filtrate and original organic layer were combined and washed with brine. Drying ($MgSO_4$) and concentration of the solution gave a solid **8** (1.10 g, 35%): mp 56−58 °C; ^1H NMR ($DCCl_3$) δ 1.25 (s, 6 H, 2 CH_3), 1.73 (t, 2 H, J = 4.8 Hz, CCH_2), 2.30 (s, 3 H, Ar−CH_3), 2.87 (s, 3 H, NCH_3), 3.19 (t, 2 H, J = 4.8 Hz, CH_2N), 6.43 (s, 1 H, Ar−H), 7.25 (s, 1 H, Ar−H); ^{13}C NMR ($DCCl_3$) δ 22.8 (Ar−CH_3), 30.8 (2 CH_3), 31.9 (Ar$C$$CH_2$), 37.0 ($CCH_2$), 39.3 ($CH_2N$), 47.5 ($NCH_3$), 110.6−144.5 (Ar−C). MS (EI) Calcd for $C_{13}H_{18}BrN$ ($M^{+\cdot}$): 267. Found: 267.

Although the above procedure was easy to perform, the modest yield of **8** was an inducement to develop an alternative method. A mixture of powdered KOH (0.732 g, 0.013 mol) in DMSO (15 mL) was stirred at 0 °C for 5 min. Lactam **6** (3.51 g, 0.013 mol) was added cautiously, followed immediately by the addition of H_3C-I (4.79 g, 0.34 mol). Stirring was continued for 0.5 h (0 °C), after which the mixture was poured into water. Extracts (H_2CCl_2, 3 × 20 mL) of the final mixture were combined, washed with water and brine, and then dried ($MgSO_4$). Evaporation of the solvent gave solid lactam **11** (2.67 g, 73%): mp 69−71 °C; IR (KBr) 1679 cm^{-1}; ^1H NMR ($DCCl_3$) δ 1.27 (s, 6 H, 2 CH_3), 2.39 (s, 3 H, Ar−CH_3), 2.48 (s, 2 H, CH_2C=O), 3.36 (s, 3 H, NCH_3), 6.86 (s, 1 H, Ar−H), 7.40 (s, 1 H, Ar−H); ^{13}C NMR ($DCCl_3$) δ 22.8 (Ar−CH_3), 27.2 (Ar$C$$CH_2$), 29.4 (2 CH_3), 32.7 (NCH_3), 45.7 (CH_2), 117.3−138.4 (Ar−C), 169.3 (C=O). MS (EI) Calcd for $C_{13}H_{14}BrNO$ ($M^{+\cdot}$): 281. Found: 281. Lactam **11** was transformed directly to **8** as follows.

Lactam **11** (4. 0 g, 0.014 mol) in dry, distilled toluene (25 mL) was cooled to 0 °C and was then treated with borane−dimethyl sulfide (2.8 mL, 0.028 mol) over 0.25 h. The mixture was stirred at 0 °C (0.25 h) and then was boiled for 2 h. After cooling to room temperature, the reaction mixture was treated with aqueous Na_2CO_3 (10%, 20 mL), and the resulting mixture was stirred for 0.5 h. Separation and drying ($MgSO_4$) of the organic layer, followed by concentration, gave **8** as an oil. Placing the oil in EtOAc (2 mL) and chilling (0 °C) overnight induced crystallization of **8** as a white solid (3.06 g, 82%), identical to that prepared above. This latter identification confirms the structure of **8**, and the procedure is a slightly more productive method.

6-Cyano-N,4,4,7-tetramethyl-1,2,3,4-tetrahydroquinoline (9). A mixture of amine **8** (2.90 g, 0.011 mol), copper(I) cyanide (1.34 g, 0.022 mol), and DMF (50 mL) was boiled vigorously for 6 h, during which time the color became dark yellow. After cooling to room temperature, the mixture was diluted with 30% aqueous NaCN (50 mL), and the resulting

solution was extracted (benzene, 4 × 30 mL). The combined extracts were dried (Na_2SO_4) and concentrated to give **9** as a light orange solid (2.13 g, 92%): mp 135−137 °C; IR (KBr) 2205 cm^{-1}; ^1H NMR ($DCCl_3$) δ 1.24 (s, 6 H, 2 CH_3), 1.70 (t, 2 H, J = 6.0 Hz, CCH_2), 2.41 (s, 3 H, Ar−CH_3), 2.96 (s, 3 H, NCH_3), 3.34 (t, 2 H, J = 6.0 Hz, CH_2N), 6.34 (s, 1 H, Ar−H), 7.32 (s, 1 H, Ar−H); ^{13}C NMR ($DCCl_3$) δ 20.5 (Ar−CH_3) 29.9 (Ar$C$$CH_2$), 31.5 (2 CH_3), 36.0 (CCH_2), 38.8 (CH_2N), 47.3 (NCH_3), 97.4 (C≡N), 110.9−147.8 (Ar−C). MS (EI) Calcd for $C_{14}H_{18}N_2$ ($M^{+\cdot}$): 214. Found: 214. Amine **9** was hydrolyzed at once to acid **10**.

***N*,4,4,7-Tetramethyl-1,2,3,4-tetrahydroquinoline-6-carboxylic Acid (10)**. A solution of nitrile **9** (0.150 g, 0.070 mmol), KOH (1.0 g), H_3C-OH (3 mL), and diethylene glycol (DEG; 5 mL) was boiled for 6 days during which time water was added on occasion to maintain volume. The reaction mixture was allowed to cool to room temperature, diluted with water (5 mL), and then acidified with concd HCl (pH ∼ 4). Extracts (H_2CCl_2, 3 × 25 mL) of the aqueous layer and the organic layer were combined, washed with water and then with brine, and finally dried (Na_2SO_4). Evaporation of the solvent gave white, solid **10** (0.062 g, 38%): mp 191−192 °C; IR (KBr) 3453−2530, 1671 cm^{-1}; ^1H NMR ($DCCl_3$) δ 1.28 (s, 6 H, 2 CH_3), 1.73 (t, 2 H, J = 6.0 Hz, CCH_2), 2.60 (s, 3 H, Ar−CH_3), 2.99 (s, 3 H, NCH_3), 3.34 (t, 2 H, J = 6.0 Hz, CH_2N), 6.34 (s, 1 H, Ar−H), 7.96 (s, 1 H, Ar−H); ^{13}C NMR ($DCCl_3$) δ 22.7 (Ar−CH_3), 30.0 (Ar$C$$CH_2$), 31.4 (2 CH_3), 36.2 (CCH_2), 38.8 (CH_2N), 47.5 (NCH_3), 112.9−148.7 (Ar−C), 163.5 (C═O). MS (EI) Calcd for $C_{14}H_{19}NO_2$ ($M^{+\cdot}$): 233. Found: 233. Acid **10** was converted to heteroarotinoid **2** without further purification.

4-Bromo-*N*-isopropylaniline (13). A mixture of **12** (1.0 g, 5.81 mmol), acetone (0.505 g, 8.7 mmol), titanium(IV) isopropoxide (1.65 g, 5.8 mmol), and ethanol (4 mL) was stirred for 12 h at room temperature. To the light brown solution was added portionwise sodium borohydride (0.439 g, 11.6 mmol) over 10 min, and then the resulting solution was stirred for 2 h. The system was cooled (0 °C) and quenched with aqueous ammonia (2 *N*, 10 mL). A precipitate formed which was filtered off and washed with ether. The filtrate was concentrated to approximately one-half volume, cooled (∼8 °C), and refiltered. Extracts of the aqueous filtrate (ether, 3 × 20 mL) were washed with brine and then dried ($MgSO_4$). Evaporation of the solvent gave an oil (0.981 g, 78%) which could be distilled (77−78 °C/2 mmHg) to give **13** as a colorless oil: IR (neat) 3407 cm^{-1}; ^1H NMR ($DCCl_3$) δ 1.17 (d, 6 H, J = 6.0 Hz, 2 CH_3), 3.45 (bs, 1 H, NH), 3.55 (m, 1 H, CH), 6.43 (dd, 2 H, Ar−H), 7.22 (dd, 2 H, Ar−H); ^{13}C NMR ($DCCl_3$) δ 22.7 (2 CH_3), 44.2 (CH), 108.3−146.4 (Ar−C). MS (EI) Calcd for $C_9H_{12}BrN$ ($M^{+\cdot}$): 213. Found: 213. Compound **13** was used directly to prepare **14**.

***N*-(4-Bromophenyl)-*N*-isopropyl-3-methyl-2-butenamide (14)**. To the biphasic solution of **13** (7.0 g, 0.033 mol), aqueous NaOH (10%, 40 mL), and H_2CCl_2 (10 mL) was added slowly 3,3-dimethylacryloyl chloride (4.65 g, 0.039 mol) in H_2CCl_2 (10 mL) over 1 h. After stirring for 24 h at room temperature, the solution was then diluted with water (20 mL), and the resulting aqueous layer was extracted (H_2CCl_2, 4 × 30 mL). The extracts were dried (Na_2SO_4) and evaporated to produce a yellow solid which was recrystallized (hexane:EtOAc, 4:1) to give **14** (6.34 g, 66%): mp 79−81 °C; IR (KBr) 1657 cm^{-1}; ^1H NMR ($DCCl_3$) δ 1.05 (d, 6 H, J = 6.8 Hz, 2 CH_3), 1.64 (s, 3 H, CH_3), 2.09 (s, 3 H, CH_3), 5.02 (m, 1 H, CH(CH_3)$_2$), 5.23 (bs, 1 H, C═CH), 6.97 (dd, 2 H, Ar−H), 7.52 (dd, 2 H, Ar−H); ^{13}C NMR ($DCCl_3$) δ 20.1 (CH_3), 21.0 (2 CH_3), 27.1 (CH_3), 45.3 (CHN), 118.2−138.1 (Ar−C), 118.2 (C=CH), 150.2 (CH_2C=CH), 166.4 (C═O). MS (EI) Calcd for $C_{14}H_{18}BrNO$ ($M^{+\cdot}$): 295. Found: 295. The amide **14** was used at once to prepare **15**.

6-Bromo-*N*-isopropyl-4,4-dimethyl-2-oxo-1,2,3,4-tetrahydroquinoline (15). A system containing **14** (5.86 g, 19.8 mmol) was heated under N_2 to 110 °C, and then $AlCl_3$ (3.96 g, 29.8 mmol) was added portionwise over 1 h. After cooling to room temperature, ice−water (∼40 mL) was added followed by H_2CCl_2 (20 mL) which dissolved a solid which had formed. The mixture was stirred (0.25 h), two layers were separated, and the aqueous layer was extracted (H_2CCl_2, 3 × 40 mL). The combined oganic extracts were washed with 10% aqueous saturated $NaHCO_3$ and brine. After drying (Na_2SO_4), the solution was concentrated to an oil (5.34 g, 96%) which was purified by chromatography (silica gel, H_2CCl_2) to give pure **15** as a light yellow oil (5.15 g, 88%); IR (KBr) 1670 cm^{-1}; ^1H NMR ($DCCl_3$) δ 1.27 (s, 6 H, 2 CH_3), 1.51 (d, 6 H, J = 7.2 Hz, 2 CH_3), 2.41 (s, 2 H, CH_2), 4.68 (m, 1 H, CH(CH_3)$_2$), 6.99 (s, 1 H, Ar−H), 7.32 (dd, 1 H, Ar−H), 7.37 (d, 1 H, Ar−H); ^{13}C NMR ($DCCl_3$) δ 20.1 (2 CH_3), 26.5 (CH(CH_3)$_2$), 32.9 (Ar$C$$CH_2$), 46.9 ($CH_2$), 48.2 ($CH$($CH_3$)$_2$), 110.1−138.6 (Ar−C), 169.5 (C═O). MS (EI) Calcd for $C_{14}H_{18}BrNO$ ($M^{+\bullet}$): 295. Found: 295. Lactam **15** was used immediately to prepare **16**.

6-Bromo-*N*-isopropyl-4,4-dimethyl-1,2,3,4-tetrahydroquinoline (16). To lactam **15** (4.0 g, 13.6 mmol) in toluene (25 mL) was added dropwise (0.25 h) borane−dimethyl sulfide (2.03 mL, 20.3 mmol). After being stirred at room temperature (1 h) and at its boiling point (1.5 h), the mixture was allowed to cool to room temperature. A solution of 10% aqueous Na_2CO_3 (20 mL) was added, and the mixture was stirred (0.5 h). Extracts (toluene) of the solution were combined, washed with brine, and dried (Na_2SO_4). Evaporation of the solvent gave a light yellow oil (3.1 g, 81%) which was chromatographed (silica gel; hexane:EtOAc, 15:1) to give **16** as a colorless oil: ^1H NMR ($DCCl_3$) δ 1.17 (d, 6 H, J = 6.4 Hz, CH(CH_3)$_2$), 1.24 (s, 6 H, 2 CH_3), 1.65 (t, 2 H, J = 6.4 Hz, CCH_2), 3.13 (t, 2 H, J = 6.4 Hz, CH_2N), 4.68 (m, 1 H, CH(CH_3)$_2$), 6.53 (d, 1 H, Ar−H), 7.10 (dd, 1 H, Ar−H), 7.22 (d, 1 H, Ar−H); ^{13}C NMR ($DCCl_3$) δ 18.6 (2 CH_3), 30.1 (CH(CH_3)$_2$), 32.2 (Ar$C$$CH_2$), 36.3 ($CH_2C$), 36.7 ($CH_2N$), 47.1 ($CH$($CH_3$)$_2$), 106.1−143.1 (Ar−C). MS (EI) Calcd for $C_{14}H_{20}NBr$ ($M^{+\bullet}$): 281. Found: 281. Amine **16** was converted directly to nitrile **17**.

6-Cyano-*N*-isopropyl-4,4-dimethyl-1,2,3,4-tetrahydroquinoline (17). A mixture of **16** (0.829 g, 2.95 mmol), copper(I) cyanide (0.528 g, 5.2 mmol), and DMF (20 mL) was boiled (24 h), after which time the resulting maroon-colored mixture was allowed to cool to room temperature. After dilution of the mixture with 30% aqueous NaCN (15 mL), the resulting solution was extracted (benzene, 3 × 30 mL), and the combined extracts were dried (Na_2SO_4). Evaporation gave an orange oil which was chromatographed (silica gel, $HCCl_3$) to give a light orange-colored oil of **17** (0.504 g, 75%): IR (KBr) 2212 cm^{-1}; ^1H NMR ($DCCl_3$) δ 1.22 (d, 6 H, J = 6.4 Hz, CH(CH_3)$_2$), 1.24 (s, 6 H, 2 CH_3), 1.66 (t, 2 H, J = 4.8 Hz, CCH_2), 3.25 (t, 2 H, J = 4.8 Hz, CH_2N), 4.14 (m, 1 H, CH(CH_3)$_2$), 6.63 (d, 1 H, Ar−H), 7.30 (dd, 1 H, Ar−H), 7.38 (d, 1 H, Ar−H); ^{13}C NMR ($DCCl_3$) δ 18.3 (2 CH_3), 29.3 (CH(CH_3)$_2$), 31.8 (Ar$C$$CH_2$), 35.6 ($CH_2C$), 36.6 ($CH_2N$), 47.4 [$CH$($CH_3$)$_2$], 95.7 (C≡N), 110.0−147.1 (Ar−C). MS (EI) Calcd for $C_{15}H_{20}BrN_2$ ($M^{+\bullet}$): 307. Found: 307. Nitrile **17** was used at once to prepare carboxylic acid **18**.

***N*-Isopropyl-4,4-dimethyl-1,2,3,4-tetrahydroquinoline-6-carboxylic Acid (18)**. A mixture of nitrile **17** (0.800 g, 3.50 mmol), KOH (3.0 g), water (3 mL), and DEG (20 mL) was boiled for 48 h, during which time water was added to maintain volume. After cooling to room temperature, the solution was diluted with water (10 mL) and then acidified with dilute HCl (pH ∼ 3). Extracts (H_2CCl_2) of the purple aqueous mixture were combined with the original organic layer, and the final solution was washed with water and then brine. After drying (Na_2SO_4), the solution was evaporated to a solid (0.495 g, 57%) which was recrystallized (EtOAc with decolorizing charcoal) to give **18** as a white solid (0.290 g, 34%): mp 184−185 °C; IR (KBr) 3443−2542, 1664 cm^{-1}; ^1H NMR ($DCCl_3$) δ 1.24 (d, 6 H, J = 6.4 Hz, CH(CH_3)$_2$), 1.29 (s, 6 H, 2 CH_3), 1.68 (t, 2 H, J = 6.4 Hz, CCH_2), 3.26 (t, 2 H, J = 6.4 Hz, CH_2N), 4.21 (m, 1 H, CH(CH_3)$_2$), 6.66 (d, 1 H, Ar−H), 7.82 (dd, 1 H, Ar−H), 7.92 (d, 1 H, Ar−H), 11.9 (s, 1 H, CO_2H); ^{13}C NMR ($DCCl_3$) δ 18.9 (2 CH_3), 29.5 (CH(CH_3)$_2$), 31.9 (Ar$C$$CH_2$), 36.0 ($CH_2C$), 36.8 ($CH_2N$), 47.4 ($CH$($CH_3$)$_2$), 109.4−148.4 (Ar−C), 172.6 (C═O). MS (EI) Calcd for $C_{15}H_{21}BrNO_2$ ($M^{+\cdot}$): 326. Found: 326. Acid **18** was converted directly to heteroarotinoid **3**.

Receptor Transactivation Assay. The receptor expression vectors pECE-hRARα/pECE-hRARβ/pECE-hRARγ and pSG5-mRXRα/pSG5-mRXRβ/pSG5-mRXRγ used in the cotransfection assay were from Magnus Pfhal (La Jolla Cancer Foundation, La Jolla, CA) and Pierre Chambon (Strasbourg, France), respectively. A basal reporter plasmid (pBL-*tk*-CAT) with a RARE from the RARβ gene placed upstream to the *tk* promoter, βRARE-*tk*-CAT, was used as the reporter plasmid in all transfection studies. The CV-1 cells were plated in 6-well culture plates at a density of 7.5×10^4 cells/well. The next day the cells were transiently transfected with plasmids consisting of a 100 ng receptor expression plasmid, 500 ng of CAT reporter plasmid (βRARE-*tk*-CAT), and 100 ng of pJAT-*Lac* (β-galactosidase) expression plasmid as internal control, using FuGENE6 transfection reagent from Boehringer Mannheim and following the manufacturer's protocol (Boehringer Mannheim Corp., Indianapolis, IN). About 16−18 h after transfection, retinoids or DMSO (solvent) was added to the cells. After incubation for 24 h, the cells were washed with phosphate-buffered saline, lysed, and assayed for CAT and βGal expression using ELISA kits from Boehringer Mannheim and following their protocols (Boehringer Mannheim Corp., Indianapolis, IN). The retinoid concentration used was in the range of 10^{-5}−10^{-10} M, and the DMSO concentration was 0.1%. All individual determinants were in triplicate and performed at least twice in separate experiments.

Growth Inhibition Assay. Cultures were plated in volumes of 150 μL in 96-well microtiter plates at concentrations of 2000−4000 cells/well, depending upon the cell line used. Retinoids were added the next day at 4X concentrations in 50 μL of media resulting in 1, 2, 4, 5, 7, and 10 mM final concentrations of each retinoid. Control cultures were treated with the same volume of DMSO. After 3 days of treatment, the cell density in each well was determined by fixing the cells in trichloroacetic acid and staining the cytoplasmic proteins with sulforhodamine B (SRB). After rinsing, the SRB was solubilized in Tris-HCl, and the optical density of each culture was determined with a MR600 microtiter plate reader. Each experiment was performed in triplicate, and the three values for each treatment were averaged. The average OD of the treated cultures was divided by that of control cultures treated with solvent alone. To determine the percent growth inhibition, this ratio was subtracted from 1 and multiplied by 100.

TGase Assay. HEL cells were plated at $(1-2) \times 10^5$ cells/mL, and the appropriate retinoid was added to give a final concentration of 10 μM. After 48 h, the cells were pelleted by centrifugation for 3 min at 1000*g*, washed twice with 127 mM NaCl, 2.7 mM KCl, 1 mM KH_2PO_4, and 8 mM Na_2HPO_4 (pH 7.4). The cell pellet was resuspended in 20 mM Tris-HCl, 150 mM NaCl, 1 mM EDTA, and 0.5 mM phenylmethanesulfonyl fluoride (pH 7.4). The cells were disrupted by a 10-s sonication, and TGase activity was measured in the sonicate by the Ca^{2+}-dependent incorporation of [1,4-^{14}C]putrescine (Amersham, Arlington Heights, IL) into *N*,*N*-dimethylcasein (Calbiochem, San Diego, CA). Radioactivity in acid-insoluble protein was determined by liquid scintillation spectrometry (Packard Instruments, Downers Grove, IL). Protein was estimated by the method of Lowry.[20]

Apoptosis Assay. The SW962 cells were plated in microtiter plates at a density of 1000 cells/well. The next day the cells were treated with a 10 μM solution of the agent or with the same volume of DMSO (solvent). After 72 h of treatment, the cells were assayed for the presence of histones in the cytoplasm using the Cell Death Detection ELISA PLUS assay acoording to the manufacturer's protocol (Boehringer Mannheim, Indianapolis, IN). The results are presented as average and standard deviations of three independent experiments performed in triplicate.

Molecular Modeling. The program Protein Data Bank is available from Brookhaven National Laboratory (Bldg 463, Brookhaven National Laboratory, Upton, NY 11973). Data for the energy of interaction (Table 2) are from five experimental runs for each flexible ligand in fixed RARγ. Similar data for the RARγ flexible receptor and flexible ligand (Table 3) were collected in two separate experiments. FlexiDock (available from Tripos, Inc., 1699 S Hanley Rd, St. Louis, MO 63144) operates on a genetic algorithm which is initiated by placing the ligand in the binding pocket of the receptor. The program then does a search of a large number of conformers which is labeled a random seed number. An evaluation of the interaction energies between the receptor and the ligand is performed, and the individual conformers are "scored". The best ligand conformers are selected for mutations in terms of variations in translational, rotational, and torsional variations with respect to the parent ligand. A similar operation is done on the receptor. These two operations then generate the flexible RARγ−flexible ligand. To explore the conformational space of the ligand, the five experiments were run with different seed and different generation numbers. The larger the generation number the higher the probability of convergence to the best interaction energies. The ligands were drawn as carboxylate anions using the fragment library of Insight Discover 97.2 (available from MSI, 9685 Scranton Rd, San Diego, CA 92121-2777). Additional information on the operations is available from the manufacturers cited.

Acknowledgment. We gratefully acknowledge partial support of this work by the National Institutes of Health through a grant from the National Cancer Institute (CA-73639). We also are pleased to acknowledge funding for the Varian Gemini 300-MHz NMR spectrometer in the Oklahoma Statewide Shared NMR Facility by the National Science Foundation (BIR-9512269), the Oklahoma State Regents for Higher Education, the W. M. Keck Foundation, and Conoco, Inc. The research was approved for publication by the Director, Oklahoma Agriculture Experiment Station and supported under Project H-1250. One of us (C.W.B.) gratefully acknowledges partial support by way of a fellowship through the NIH Minorities in Biomedical Research, Grant 5 R25 GM55244-02.

References

(1) (a) Armstrong, R. B.; Ashenfelter, K. O.; Eckhoff, C.; Levin, A. A.; Shapiro, S. S. In *The Retinoids- Biology, Chemistry, and Medicine*, 2nd ed.; Sporn, M. B., Roberts, A. B., Goodman, D. S., Eds., Raven Press: New York, 1994; Chapter 13, pp 545−572. (b) Dawson, M. I. In *Burger's Medicinal Chemistry and Drug Discovery*, 5th ed.; Burger, A., Ed.; Wiley: New York, 1996; Chapter 44, pp 631−658.

(2) Frolik, C. A. In *The Retinoids, Vol. 2*; Sporn, M. B., Roberts, A. B., Goodman, D. S., Eds.; Academic Press: Orlando, FL, 1984; Chapter 11, pp 177−208.

(3) (a) Benbrook, D. M.; Madler, M. M.; Spruce, L. W.; Birckbichler, P. J.; Nelson, E. C.; Subramanian, S.; Weerasekare, G. M.; Gale, J. B.; Patterson, Jr., M. K.; Wang, B.; Wang, W.; Lu, S.; Rowland, T. C.; DiSevestro, P.; Lindamood, III, C.; Hill, D. L.; Berlin, K. D. Biologically Active Heteroarotinoids Exhibit Anticancer Activity and Decreased Toxicity. *J. Med. Chem*. **1997**, *40*, 3567−3583. (b) Benbrook, D. M.; Subramanian, S.; Gale, J. B.; Liu, S.; Brown, C. W.; Boehm, M. F.; Berlin, K. D. Synthesis and Characterization of Heteroarotinoids Demonstrates Structure−Activity Relationships. *J. Med. Chem*. **1998**, *41*, 3753−3757. (c) Lindamood, III, C.; Giles, H. D.; Hill, D. L. Preliminary Profile of Arotinoids SMR-2 and SMR-6 in male B6D2F1 Mice. *Fundam. Appl. Toxicol*. **1987**, *8*, 517−530. (d) Lindamood, III, C.; Dillehay, D. L.; Lamon, E. W.; Giles, H. D.; Shealy, Y. F.; Sani, B. P.; Hill, D. L. Toxicologic and Immunologic Evaluations of *N*-(All-*trans*-Retinoyl)-*d*,*l*-Leucine and *N*-(All-*trans*-Retinoyl)glycine. *Toxicol. Appl. Pharmacol*. **1988**, *96*, 279−295.

(4) (a) Beard, R. L.; Chandraratna, R. A. S.; Colon, D. F.; Gillett, S. J.; Henry, E.; Marler, D. K.; Song, T.; Denys, L.; Garst, M. E.; Arefieg, T.; Klein, E.; Gil, D. W.; Wheeler, L.; Kochhar, D. M.; Davies, P. J. A. Synthesis and Structure−Activity Relationships of Stilbene Retinoid Analogues Substituted with Heteroaromatic Carboxylic Acids. *J. Med. Chem*. **1995**, *38*, 2820−2829. (b) Beard, R. L.; Colon, D. F.; Song, T. K.; Davies, P. J. A.; Kochhar, D. M.; Chandraratna, R. A. S. Synthesis and Structure−Activity Relationships of Retinoid X Receptor Selective Diaryl Sulfide Analogues of Retinoic Acid. *J. Med. Chem*. **1996**, *39*, 3556−3563.

(5) (a) Boehm, M. F.; McClurg, M. R.; Pathirana, C.; Manglesdorf, D.; White, S. K.; Herbert, J.; Winn, D.; Goldman, M. E.; Heyman, R. A. Synthesis of High Specific Activity [^{3}H]-9-*cis*-Retinoic Acid and Its Application for Identifying Retinoids with Unusual Binding Properties. *J. Med. Chem*. **1994**, *37*, 408−414. (b) Boehm, M. F.; Zhang, L.; Badea, B. A.; White, S. K.; Mais, D. E.; Berger, E.; Suto, C. M.; Goldman, M. E.; Heyman, R. A. Synthesis and Structure−Activity Relationships of Novel Retinoid X Receptor-Selective Retinoids. *J. Med. Chem*. **1994**, *37*, 2930−2941.

(6) Gale, J. B. Recent Advances in the Chemistry and Biology of Retinoids. In *Progress in Medicinal Chemistry*, *Vol. 30*; Ellis, G. P., Luscombe, D. K., Eds.; Elsevier Science Publishers B.V.: Amsterdam, 1993.

(7) Lehmann, J. M.; Dawson, M. I.; Hobbs, P. D.; Husmann, M.; Pfahl, M. Identification of Retinoids with Nuclear Receptor Subtype-Selective Activities. *Cancer Res*. **1991**, *51*, 4803−4809.

(8) Warrell, Jr., R. P.; Frankel, S. R.; Miller, Jr., W. H.; Scheinberg, A.; Jakubowski, A. Differentiation Therapy of Acute Promyelocytic Leukemia With Tretinoin (all *trans*-Retinoic Acid). *N. Engl. J. Med*. **1991**, *324*, 1385−1393.

(9) (a) Suedhoff, T.; Birckbichler, P. J.; Lee, K. N.; Conway, E.; Patterson, Jr., M. K. Expression of Transglutaminase in Human Erythroleukemia Cells in Response to Retinoic Acid. *Cancer Res*. **1990**, *50*, 7830−7834. (b) Jacob, K.; Wach, F.; Holzapfel, U.; Hein, R.; Lengyel, E.; Buettner, R.; Bosserholl, A. K. In Vitro Modulation of Human Melanoma Cell Invasion and Proliferation by All-*trans*-Retinoic Acid. *Melanoma Res*. **1998**, *8*, 211−219. (c) Waliszewski, P.; Waliszewska, M. K.; Gordon, N.; Hurst, R. E.; Benbrook, D. M.; Dhar, A.; Hemstreet, G. P. Retinoid Signaling in Immortalized and Carcinoma-Derived Human Uroepithelial Cells. *Mol. Cell. Endrocrinol*. **1999**, *148*, 55−65.

(10) Birckbichler, P. J.; Patterson, Jr., M. K. Growth Regulation by Products From Cells. *Technol. Cell Biol*. **1985**, *C1*, 1−20.

(11) Birckbichler, P. J.; Patterson, Jr., M. K. Modulation of Transglutaminase-Catalyzed Isopeptide Bonds in Human Cells In *Hemostatis and Cancer*; Muszbeck, L., Ed.; CRC Press: Boca Raton, FL, 1987.

(12) (a) Oridate, N.; Lotan, D.; Mitchell, M. F.; Hong, W. K.; Lotan, R. Inhibition of Proliferation and Induction of Apoptosis in Cervical Carcinoma Cells by Retinoids. Implication for Chemoprevention. *J. Cell Biochem*. **1995**, *Suppl. 23*, 80−86. (b) Oridate, N.; Lotan, D.; Xu, X.-C.; Hong, W. K.; Lotan, R. Differential Induction of Apoptosis by All-*trans*-Retinoic Acid and *N*-(4-Hydroxyphenyl)retinamide in Human Head and Neck Squamous Cell Carcinoma Cell Lines. *Clin. Cancer Res*. **1996**, *2*, 855−863. (c) Oridate, N.; Higuchi, M.; Suzuki, S.; Shroot, B.; Hong, W. K.; Lotan, R. Rapid Induction of Apoptosis in Human C33-A Cervical Cell Carcinoma Cells by the Synthetic Retinoid 6-[3-(1- adamantyl)hydroxyphenyl]-2-naphthalene Carboxylic Acid (CD437). *Int. J. Cancer* **1997**, *70*, 484−487.

(13) Zhang, X.-k.; Lehmann, J.; Hoffmann, B.; Dawson, M. I.; Cameron, J.; Graupner, G.; Hermann, T.; Tran, P.; Pfahl, M. Homodimer Formation of Retinoid X Receptor Induced by 9-*cis*-Retinoic Acid. *Nature* **1992**, *358*, 587−5891.

(14) Look, J.; Landwehr, J.; Bauer, F.; Hoffman, A. S.; Bluethmann, H.; Lemotte, P. Marked Resistance of RARγ-Deficient Mice to The Toxic Effects of Retinoic Acid. *Am. J. Physiol*. **1995**, *269*, E91−E98.

(15) Chen, S.; Ostrowski, J.; Whiting, G.; Roalsvig, T.; Hammer, L.; Currier, S. J.; Honeyman, J.; Kwasniewski, B.; Sterzycki, R.; Kim, C. U.; Starrett, J.; Mansuri, M.; Reczek, P. R. Retinoic Acid Receptor Gamma Mediates Topical Retinoid Efficacy and Irritation In Animal Models. *J. Invest. Dermatol*. **1995**, *104*, 779−783.

(16) Renauld, J.-P.; Rochel, R.; Ruff, R.; Vivat, V.; Chambon, P.; Gronemeyer, H.; Moras, D. Crystal Structure of the RAR-γ Ligand Binding Domain Bound to All-*Trans*-Retinoic Acid. *Nature* **1995**, *378*, 681−689.

(17) Bourguet, W.; Ruff, M.; Chambon, P.; Gronemeyer, H.; Moras, D. Crystal Structure of the Ligand-Binding Domain of Human Nuclear Receptor RXR-α. *Nature* **1995**, *375*, 377−382.

(18) Wurtz, J. M.; Borguet, W.; Renauld, J. P. Vivat, V.; Chambon, P.; Moras, D.; Gronemeyer, H. A Canonical Structure for the Ligand-Binding Domain of Nuclear Receptors. *Nature Struct. Biol*. **1996**, *3*, 87−94.

(19) Caelles, C.; Gonzalez-Sancho, J. M.; Munoz, A. Nuclear Hormone Receptor Antagonism with AP-1 by Inhibition of the JNK Pathway. *Genes Devel*. **1997**, *11*, 3351−3364.

(20) Fisher, G. J.; Talwar, H. T.; Wang, Z. Q.; McPhillips, F.; Madore, S.; Voorhees, J. J. Retinoic Acid Antagonizes Activation of Transcription Factor AP-1 by Ultraviolet Irradiation Through a Novel Mechanism in Human Skin In Vivo: Inhibition of c-JUN Protein Expression. *J. Invest. Dermatol*. **1997**, *108*, 578 (Abstract).

(21) Yen, A.; Roberson, M. S.; Varyvayanis, S.; Lee, A. T. Retinoic Acid-Induced Mitogen-Activated Protein (MAO)/Extracellular Signal-Regulated Kinase (ERK) Kinase-Dependent MAP Kinase Activation Needed to Elicit HL-60 Cell Differentiation and Growth Arrest. *Cancer Res*. **1998**, *58*, 3163−3172.

(22) Zelent, A.; Krust, A.; Petkovich, M.; Kastner, P.; Chambon, P. Cloning of Murine α and β Retinoic Acid Receptors and a Novel Receptor γ Predominately Expressed in Skin. *Nature* **1989**, *339*, 714−717.

(23) Pfahl, M.; Apfel, R.; Bendrik, I. Nuclear Retinoid Receptors and Their Mechanism of Action. In *Vitamins and Hormones*; Litwack, G., Ed.; Academic Press: San Diego, CA, 1994; pp 327−382.

(24) Boehm, M. F.; Zhang, L.; Zhi, L.; McClurg, M. R.; Berger, E.; Wagoner, M.; Mais, D. E.; Suto, C. M.; Davies, P. J. A.; Heyman, R. A.; Nadzan, A. M. Design and Synthesis of Potent Retinoid X Receptor Selective Ligands That Induce Apoptosis in Leukemia Cells. *J. Med. Chem*. **1995**, *38*, 3146−3155.

(25) Zhang, L.-X.; Mills, K. J.; Dawson, M. I.; Collins, S. J.; Jetten, A. M. Evidence For The Involvement of Retinoic Acid Receptor RARα-Dependent Signaling Pathway in the Induction of Tissue Transglutaminase and Apoptosis By Retinoids. *J. Biol. Chem*. **1995**, *270*, 6022−6029.

(26) Bernard, B. A.; Bernardon, J. M.; Delescluse, C.; Martin, B.; Lenoir, M.-C.; Maignan, J.; Charpentier, B.; Pilgrim, W. R.; Reichert, U.; Shroot, B. Identification of Synthetic Retinoids With Selectivity for Human Nuclear Retinoic Acid Receptor γ. *Biochem. Biophys. Res. Commun*. **1992**, *186*, 977−983.

(27) Klaholz, B. P.; Renauld, J.-P.; Mitschler, A.; Zuis, C.; Chambon, P.; Gronemeyer, H.; Moras, D. Conformational Adaptation of Agonists to the Human Nuclear Receptor RARγ. *Nature Struct. Biol*. **1998**, *5*, 013−016.

(28) (a) Kagechika, H.; Kawachi, E.; Hashimoto, Y.; Himi, T.; Shudo, K. Retinobenzoic Acids. 1. Structure-Activity Relationships of Aromatic Amides With Retinoidal Activity. *J. Med. Chem*. **1988**, *31*, 2182−2192. (b) Kagechika, H.; Himi, T.; Kawachi, E.; Hashimoto, Y.; Shudo, K. Retinobenzoic Acids. 4. Conformation of Aromatic Amides With Retinoidal Activity. Importance of *trans*-Amide Structure for the Activity. *J. Med. Chem*. **1989**, *32*, 2292−2296.

(29) Jones, P.; Villeneuve, G. B.; Fei, C.; DeMarte, J.; Haggatary, A. J.; Nwe, K. T.; Martin, D. A.; Lebuis, A.-M.; Finkelstein, J. M.; Gour-Salin, B. J.; Chan, T. H.; Leyland-Jones, B. R. Synthesis and Structure-Activity Relationships of 2-Pyrazinylcarboxamidobenzoates and β-Ionylideneacetamidobenzoates With Retinoidal Activity. *J. Med. Chem*. **1998**, *41*, 3062−3077.

JM9900974